Molecular mechanisms of the regulation of ATPase cycle in striated muscle

Yuri S. Borovikov[1], Olga E. Karpicheva[1] & Charles S. Redwood[2]
[1]Institute of Cytology of Russian Academy of Sciences, Tikhoretsky 4, 194064 St. Petersburg, Russia. [2]Department of Cardiovascular Medicine, University of Oxford, Oxford OX3 7BN, UK.

New data on the molecular mechanism of the regulation of ATPase cycle by troponin-tropomyosin system have been obtained in reconstructed muscle fibers by using the polarized fluorescence technique, which allowed us following the azimuthal movements of tropomyosin, actin subdomain-1 and myosin SH1 helix motor domain during the sequential steps of ATPase cycle. We found that tropomyosin strands "rolling" on thin filament surface from periphery to center at ATPase cycle increases the amplitudes of multistep changes in special arrangement of SH1 helix and subdomain-1 at force generation states. These changes seem to convey to actin monomers and to myosin "lever arm", resulting in enhance of the effectiveness of each cross-bridge work. At high-Ca^{2+} troponin, a shift of tropomyosin strands further to center at strong-binding states increases this effect. At low-Ca^{2+} troponin "freezes" tropomyosin and actin in states typical for weak-binding states, resulting in disturbing the teamwork of actin and myosin.

Muscle contraction is generated by the interaction of myosin cross-bridges with actin filaments and ATP. During force generation, the cycle of myosin cross-bridges passes through several conformational states, the so-called ‘‘strong’’ and ‘‘weak’’ forms of myosin binding to actin[1]. In striated muscle, the interaction of myosin with actin is regulated by tropomyosin (TM) and troponin (TN) on actin filaments in response to a change in Ca^{2+} concentration. Both structural and biochemical data suggest that TM can occupy three different positions on actin ("blocked" or calcium-free; "closed" or calcium induced; and myosin induced or "open"), depending on the presence or absence of troponin, myosin, and Ca^{2+} [2-5]. It is suggested that in the "blocked" position, TM sterically blocks the specific myosin-binding site on the actin filament, resulting in an inhibition of the actomyosin interaction[6,7]. The binding of Ca^{2+} to TN removes this inhibition by azimuthal movement of TM strands, allowing myosin to interact freely with actin[3]. The isomerization of myosin heads to a strong complex with F-actin shifts TM further to the periphery of thin filaments, to "open" state[8]. While these tropomyosin movements are well established, the molecular mechanism of regulation of actin-myosin interaction by troponin-tropomyosin complex during ATPase cycle is an open and intriguing question.

Polarized fluorimetry is a highly sensitive method for studying conformational changes of contractile proteins in muscle fibers[9,10]. Using this method, has shown previously that the formation of strong-binding of myosin to actin in the muscle fiber induces the change in a tilt angle of myosin motor domain (or SH1 helix)[11-14], in a rotation of myosin "lever arm"[15,16], and in a shift of subdomain-1 and subdomain-2 of actin[17]. The observed was potentiation of the inhibitory action of troponin I by tropomyosin[18]. Interaction of S1 with actin resulted in nucleotide-dependent displacement of smooth tropomyosin and changes in its mobility on thin filaments[19]. The aim of the present work was to investigate by this method the mutual effect of TN and Ca^{2+} on the mobility and the movements of tropomyosin, actin subdomain-1 and SH1 helix of myosin catalytic domain during the sequential steps of the actomyosin ATPase cycle in a skeletal ghost fiber. The strength of actin binding to myosin during each step was determined by the addition of a respective nucleotide.

In this work, we used a well-organized model system of thin filaments reconstituted in skeletal muscle ghost fibers[20,21] from fluorescently labeled exogenous g-actin, S1 and TM in the absence or presence of TN and Ca^{2+}. Fluorescence labels were covalently linked to the cystein residues of proteins: 1.5-IAEDANS to Cys374 of subdomain-1 of actin (Actin-IAEDANS) or to Cys707 of motor domain of myosin subfragment-1 (S1-IAEDANS) and 5-IAF to Cys190 or

Cys36 of TM (TM-IAF). The parameters of polarized fluorescence (N and Φ_E) from these fluorescent probes have been determined at modeling various intermediate states of the ATPase cycle (Fig. 1, 2). According to the data obtained previously[17,19,21], the alteration in the relative number of disordered probes (N) and in the angle of emission dipole (Φ_E) of dyes, were interpreted as the changes in the mobility and in the orientation of probe-containing regions namely: myosin SH1 helix, actin subdomain-1 and N- and C-terminus of TM. All changes of the values of N and Φ_E were statistically significant ($p < 0.05$) and reversible. Since the modification of the cystein residues does not affect the functional properties of these proteins[13,22,23], it is possible to suggest that the movements of SH1 helix, actin subdomain-1 and TM strands on thin filament surface take place during the ATPase cycle in native muscle fiber.

The transformation from AM.ADP.P_i to the rigor state is accompanied by multistep decrease of N and Φ_E from 1.5-IAEDANS attached to motor domain, which indicates that the transition from weak to strong states of myosin binding produces a discrete increase of myosin affinity to actin and the multistep shift of SH1 helix to the thin filament axis (Fig 1a, b). At the transition from AM.ADP.P_i to the rigor, the fraction of disoriented fluorophores rose by 28% (Fig. 1b) and the angle Φ_E decreased approximately by 7º (Fig. 1a). Similar amplitude of movements of SH1 helix at the ATPase cycle has been suggested earlier[24]. It is interesting that most changes of polarized parameters (N and Φ_E) were observed between the stages A.M*·ATP (mimicked by MgATPγS) and A.M^ADP (mimicked by MgADP), i.e., at the ATPase cycle area, at which the generation of force by actomyosin motor seems to occur[25]. It is not ruled out that the closure of the myosin nucleotide-binding cleft at ATPase cycle[25,26] leads to a change of spatial organization of the SH1 helix and to subsequent transduction of these changes to the myosin "lever arm"[27,28].

The muscle contraction was accompanied by a change in the orientation of actin monomers in thin filaments[17,21,29,30]; each intermediate state of the ATPase cycle myosin corresponded to a certain orientation of actin monomers and rigidity of thin filaments[21]. In the present work, it is shown that each myosin intermediate state also corresponds to a certain spatial organization of subdomain-1 of actin monomer and its mobility (Fig. 1c, d). The transition from weak- to strong-binding states induces a decrease of N and an increase of Φ_E of 1.5-IAEDANS attached to the subdomain-1 (Fig. 1b), which indicates the rotation of this subdomain from the filament center (Fig. 1d) and its mobilization by S1[17]. At the same time, greater shift of myosin SH1 helix corresponds to greater shift of actin subdomain-1 (Fig. 1a, c).

At the transition from AM.ADP.P_i to the rigor, fraction of disoriented fluorophores bound to actin, N decreased by 10% (Fig. 1d) and the angle Φ_E rose by 8º (Fig. 1c). Like for S1, most pronounced changes of mobility and orientation of fluorophores were observed between the stages A.M*·ATP and A.M^ADP, i.e., at the intermediate states, at which the force generation by actomyosin motor seems to occur[25]. Hence, ATPase cycle was accompanied by multistep and interdependent changes in the myosin and actin conformational states.

It is widely believed that ionic and hydrophobic residues that are possibly involved in actin binding are localized at one end of the myosin head in the so-called "actin-binding" cleft, which is far either from the enzyme pocket or from the converter. Since the enzyme pocket was connected to the apex of the cleft, actin binding caused the cleft closure, resulting in opening the enzyme pocket and acceleration of product release. The myosin head has an enzyme pocket in which ATP hydrolysis occurs, a long, stiff α-helix ("relay helix") to transmit linear force, a converter to turn it into a rotation, and a myosin lever arm to deliver a mechanical impulse to actins[25,28]. Our data indicate that the changes at the myosin active site are transmitted not only to the SH1 helix located close to a converter, but also to actin, producing nucleotide-dependent changes of mobility and position of subdomain-1 in thin filaments (Fig. 1c, d). Besides, the conformational changes in subdomain-1 seem to be transmitted to neighboring actin monomer[17], producing cooperative changes of thin filament rigidity and the changes in actin monomer orientation[17,21,29,30].

It is accepted that at initial stages of the ATPase cycle the myosin head is bound to one actin monomer and forms a weak-binding state. Then the myosin head, after a series of conformational changes, binds to one more of the neighboring actin monomers, the area of the binding site increases with each step of ATPase cycle[25]. Our data do not contradict such suggestion. At the transition from AM.ADP.P_i to the rigor state, there occurs a multistep increase of the strength of myosin binding to actin and a consecutive shift of subdomain-1 to the filament axis (Fig. 1c, d). Since actin small domain contains the strong myosin binding site[25], we can suggested that the cause of the increase of the strength of this binding (affinity) is an enhancement of stereospecific and hydrophobic interaction between actin and myosin molecules; such change of configuration of the myosin-binding site occurs at the shift of subdomain-1 from the center of filament. If our suggestion is correct, then the more subdomain-1 shifting to the periphery of filament axis will correlate with the more essential rise of the strength of myosin-binding to actin and with the more pronounced movement of SH1 helix to the center of a thin filament. In this case, maximum movements of the SH1 helix and actin subdomain-1 can be expected at rigor state. Such effect has been observed in our experiments (Fig. 1).

As follows from Fig. 1c, d, TM produces an essential effect on mobility and spatial arrangement of actin subdomain-1. It was shown previously, that TM induces the changes in conformation of actin[18]. The conformational changes are accompanied by an increase of actomyosin ATPase activity[31,32], of the force in single thin filaments[33], and of the force supported by cross-bridges[34]. According to the data presented in Fig. 1, TM affects markedly the formation of strong- and weak-binding of S1 to actin. This indicates the TM-induced changes in the conformational state of the myosin motor domain and of the actin subdomain-1, which have been revealed at modeling various intermediate states of the ATPase cycle. Thus, in the presence of MgADP, the values of N and Φ_E from probes attached to SH1 helix and the actin subdomain-1 turned out to be close to the values of these parameters observed in the absence of TM at modeling rigor state, i.e., at formation of the more strong-binding state. The greatest changes of N and Φ_E were observed between the stages A.M*·ATP and A.M^ADP (Fig 2,a-d), i.e., at the states, where the generation of force by actomyosin motor occurs[25].

TM increased the SH1 helix movement amplitude by 22% at the transition from AM.ADP.P_i to the rigor state (Fig. 1a). Since the change in the SH1 helix position seems to be transited to the myosin "lever arm" whose rotation is thought to be the key role in the development of force[25,35,36], the increase of amplitude of SH1 helix movements in the ATPase cycle indicates that TM increases the efficiency of work of each cross-bridge. Such TM effect has been recently revealed[34]. The authors explained the increase of work of each cross-bridge by the partially modified actin configuration so as to enhance stereospecific and hydrophobic interaction between actin and myosin molecules. Since the strong myosin binding site is located at the small domain of actin[25], it can be suggested that the enhancement of the stereospecific and hydrophobic interaction between actin and myosin molecules is a result of an increase of the area of hydrophobic interaction between actin and myosin molecules[37], which occurs due to an additional shift of subdomain-1 from the center of filament axis (Fig. 1g, h).

The modulation of actin-myosin interaction at ATPase cycle by TM seems to be realized by a shift or "rolling"[38] of the tropomyosin strand on the thin filament surface. Such conclusion follows from the data of Fig. 1e. It is known that the nucleotide-free myosin head, binding with actin, shifts TM to the filament center[8]. Our data indicate that S1 shifts TM in the nucleotide-dependent manner. According to the data presented in Fig. 1e, the transformation from weak- to strong-binding states produces a multistep shift of TM from the periphery to the filament center. Such shift is accompanied by a multistep decrease of the TM molecule flexibility. At transition from weak- to strong-binding states, the values of N decreased by 35% (Fig. 1f). A reduction of pool of disorder molecules of the dye localized on TM is easy to be explained by an increase of the strength of binding of this protein to actin[19]. As follows from Fig. 1, TM by "rolling" on the thin filament surface modifies S1-dependent structural changes in actin, the strength of its binding with myosin, and the conformational changes in myosin initiated by this binding. There

seems to be preserved the concerted and interdependent conformational changes in actin and myosin.

TN modulates in a Ca^{2+}-dependent manner the TM effect by changing the conformation of actin and TM[39,40]. According to Fig. 2, at high-Ca^{2+} TN enhances the effect of TM in the absence of nucleotide and in the presence of MgADP, i.e., at the formation of strong-binding states. Thus, the values of N and Φ_E of SH1 and subdimain-1 in the presence of MgADP turn out to be close to the values observed at modeling rigor state in the absence of TN (Fig. 2a-d). In contrast, the modeling by of MgATPγS of the weak-binding state is accompanied by the appearance of the parameters that were observed in the absence of TN at modeling by MgATP of the weaker binding state (Fig. 2a-d). Hence, TN and high-Ca^{2+} shift the formation of the strong- and weak-bindings towards the stronger and the weaker binding states, respectively.

TN and high-Ca^{2+} rise the movement amplitude of SH1 helix and actin subdomain-1 at transition from weak- to strong-binding states by 71% and 3% (Fig. 2a, c), respectively. Since at high-Ca^{2+}, TN causes an additional shift of actin subdomain-1 from the filament center (Fig. 2g), it can be expected that the enhancement of stereospecific and hydrophobic interaction between actin and myosin molecules will increase the efficiency of actomyosin motor in the presence of TN and high-Ca^{2+}. Such conclusion does disagree with the recently obtained data indicating that the tension of each cross-bridge increase by 14% in the presence of TN and high-Ca^{2+} [34].

At modeling ATPase cycle in the presence of TN and high-Ca^{2+}, there were observed the movements of tropomyosin on thin filaments surface (Fig. 2e). The tropomyosin strands were shifted as compared with its position in the absence of TN further to the center and then to the filament periphery at the formation of strong- and weak-binding forms, respectively (Fig. 2e, g). The amplitude of this shift increases by 22%. This indicates that the activation of work of each cross-bridge correlates with an increase of amplitude of the shift of TM on the thin filament surface.

In contrast, at low-Ca^{2+}, TN inhibits "rolling" of TM, the shift of SH1 helix and the rotation of subdomain-1 in the ATPase cycle (Fig. 2). It was shown previously that TN-I, binding to actin, produces a shift of subdomain-1 to the thin filament periphery[18], which seems to reduce the area of stereospecific and hydrophobic interaction between actin and myosin molecules. A decrease of this area leads to the inhibition of strong-binding S1 and actin. TM activates this effect[18]. The data obtained in the present work indicate that at low-Ca^{2+}, TN shifts all intermediate states of the ATPase cycle towards the formation of the weaker binding (Fig. 2). Thus, in the absence of nucleotide and in the presence of MgADP, MgANP-PNP or MgATPγS, the mobility and spatial arrangement of SH1 helix approached to these observed in the presence of MgANP-PNP, MgATPγS or MgATP, i.e., at the formation of the weaker binding states. This shift produces a weak effect on the amplitude of the SH1 helix movements at transformation from weak- to strong-binding states (Fig. 2a). In contrast, there was revealed a marked inhibition of movement amplitude of subdomain-1 at transition from weak- to strong-binding states (by 12%) (Fig. 2c). Even in the absence of nucleotides and in the presence of MgADP, only slight changes in mobility and in rotation of subdomain-1 has been found, which typical for the formation of weak-binding forms at stages close to A*M*ATP or A**M**˙ADP˙P_i (Fig. 2c, d). It is possible that at low-Ca^{2+}, the TM-TN complex is able to stop the ATP hydrolysis cycle, "freezing" actomyosin in weak-binding states.

Inhibition of the ATPase cycle seems to occur with an active participation of tropomyosin, because at low-Ca^{2+} even at modeling strong-binding states, TM occupies the position typical for weak-binding states and the amplitude of TM movements decreases markedly (by 22%). Hence, uncoupling of interdependent conformational changes in myosin and actin during the ATPase cycle occurs due to "freezing" of myosin-dependent TM band movements (Fig. 2e) and transforms actin conformation to "OFF" state (Fig. 2h).

Resembling results we observed when the αα-TM specifically modified by the fluorescent probe with Cys190 was used (data not shown). It means that there no essential

difference between the molecular mechanism of regulation of ATPase cycle induced by either ββ-TM and αα-TM.

It is interesting, that the disturbing of the team-work of actin and myosin, which correlated with inhibition of the actin-activated ATPase activity, has been revealed in our previous studies on the mechanisms of the ATPase cycle regulation by such smooth muscle regulatory protein as caldesmon[19,21]. In this case, the regulatory protein inhibited the ATPase cycle of "freezing" the myosin-dependent TM movements and the actin structural state in the "OFF" states. It seems that for different muscle tissues, there exist the similar mechanisms of inhibition of interaction of myosin and actin in the ATPase cycle, which is realized by the disturbing of the team-work of actin and myosin.

Thus, our results provide strong evidence to support the suggestion the interdependent and multistep conformational changes of myosin and actin at muscle contraction[1,25,41]. These conformational changes seem to be accompanied by the changes in orientation and mobility of actin subdomain-1 and myosin SH1 helix at the ATPase cycle, which are transferred to neighboring actin monomers[17] and to myosin light-chain region during force generation[25,36]. In the ATPase cycle, TM, "rolling" in a myosin-dependent manner from periphery to the centre on the thin filament surface, increases the amplitude of the changes in spatial organization of subdomain-1 and SH1 helix and, it is possible, in such a way enhances team-work of the each cross-bridge. TN modulates this effect of TM. At high-Ca^{2+}, TN shifts TM to the centre and the periphery of thin filament at the formation of the strong- and weak-binding, respectively, and enhances team-work of each cross-bridge. At low-Ca^{2+}, TN inhibits ATPase cycle by "freezing" myosin-dependent movements TM and actin conformation in "OFF" states.

METHODS SUMMARY

Ghost fibers, myosin subfragment-1 (S1), g-actin and wild-type human troponin complex and αα- and ββ-tropomyosins were prepared as described in Methods section. G-actin and S1 was labeled at Cys707 and at Cys374, respectively, using N-iodoacetyl-N′-(5-sulfo-1-naphtylo)ethylenediamine (1.5-IAEDANS)[12, 42] and wild-type human αα- and ββ-tropomyosins labeled at Cys190 or Cys36, using 5-iodoacetamide fluorescein (5-IAF)[19,22]. The reconstruction of regulated thin filaments has been described in detail previously[20,21]. The molar ratio of S1, tropomyosin and troponin to actin in the muscle fibers was 1:5 (±2), 1:6.5 (±2) and 1:6,5 (±1), respectively. The polarized fluorescence from 1.5-IAEDANS and 5-IAF was registered at 500–600 nm after excitation at 365±5 nm and 437±5 nm, respectively. The intensities of the four components of polarized fluorescence were measured parallel ($_{\parallel}I_{\parallel}$, $_{\parallel}I_{\perp}$) and in perpendicular ($_{\perp}I_{\perp}$, $_{\perp}I_{\parallel}$) to the fiber axis relative to the polarization plane of the exiting light using a photometer[17] and a probe orientation was calculated using model-dependent and model independent methods[17,43], in view of the ordered probes lies at angles Φ_A and Φ_E with respect to fiber axis for absorption ($\vec{A}$) and emission ($\vec{E}$) dipoles, respectively and N is completely disordered probes. The significance of the data differences observed was determined by Student's t-test.

Full Methods and any associated reference are available in the online version of the paper at www.nature.com/nature.

Figure 1 | Fluorescence polarization parameters Φ_E and N from IAEDANS probes on myosin SH1 helix and actin subdomain-1 and from IAF on tropomyosin at modeling of ATPase cycle. The measurement of polarized fluorescence was carried out in the buffer containing in mM: 10 KCl, 3 $MgCl_2$, 1 DTT, 4 EGTA (or 0.1 $CaCl_2$), 6.7 phosphate buffer, pH 7.0, in the absence or presence of 2.5 ADP, 25 AMP-PNP, 10 ATPγS or 5 ATP[21]. The absence of nucleotide mimicked the AM state of the actomyosin complex. MgADP, MgAMP-PNP, MgATPγS and MgATP were used to mimic A.M^ADP, A.M**.ATP and A.M*·ATP states[44,45], respectively. The relative number of disordered probes (N), the angles of orientation absorption

(Φ_A) and emission (Φ_E) dipoles were calculated using model-dependent[43] and model-independent methods[17]. Since in all experiments the values of this parameter were similar for both methods and the pattern of the changes in Φ_E was similar to those in Φ_A, only Φ_E values calculated with model dependent method were presented. **a**, **b**, **c** and **d**, **e**, **f,** The values of Φ_E and N for SH1 helix, subdomain-1 and tropomyosin at modeling different intermediates ATPase cycle, respectively. All changes of Φ_E and N were statistically significant ($P<0.005$). **g, h,** Simple models of actin-myosin interaction at ATPase cycle in the absence or presence of tropomyosin, respectively.

Figure 2 | The effect of troponin and Ca^{2+} on fluorescence polarization parameters Φ_E and N from IAEDANS probes on myosin SH1 helix, actin subdomain-1 and IAF on tropomyosin at modeling of ATPase cycle. The conditions of the measurements were as in Fig. 1. **a**, **b**, **c** and **d**, **e**, **f,** The values of Φ_E and N for SH1 helix, subdomain-1 and tropomyosin at modeling different intermediates ATPase cycle, respectively. All changes of Φ_E and N was statistical significance ($P<0.005$). **g, h,** Simple models of actin-myosin interaction and tropomyosin position at ATPase cycle in high- and low-Ca^{2+}, respectively.

References

1. Lymn, R. W. & Taylor, E. W. Mechanism of adenosine triphosphate hydrolysis by actomyosin. *Biochemistry* **10**, 4617-4624 (1971).
2. McKillop, D. F. & Geeves, M. A. Regulation of the interaction between actin and myosin subfragment 1: evidence for three states of the thin filament. *Biophys. J.* **65**, 693–701 (1993).
3. Lehman, W., Vibert, P., Uman, P. & Craig, R. Steric-blocking by tropomyosin visualized in relaxed vertebrate muscle thin filaments. *J. Mol. Biol.* **251**, 191–196 (1995).
4. Vibert, P., Craig, R. & Lehman, W. Steric-model for activation of muscle thin filaments. *J. Mol. Biol.* **266**, 8-14 (1997).
5. Maytum, R., Lehrer, S. S. & Geeves, M. A. Cooperativity and switching within the three-state model of muscle regulation. *Biochemistry* **38**, 1102-1110 (1999).
6. Haselgrove, J. C. & Huxley, H. E. X-ray evidence for radial cross-bridge movement and for the sliding filament model in actively contracting skeletal muscle. *J. Mol. Biol.* **77**, 549-568 (1973).
7. Huxley, H. E. Muscular contraction and cell motility. Nature 243, 445-449 (1973).
8. Craig, R. & Lehman, W. Crossbridge and tropomyosin positions observed in native, interacting thick and thin filaments. *J. Mol. Biol.* **311**, 1027–1036 (2001).
9. Borovikov, Y. S. Conformational changes of contractile proteins and their role in muscle contraction. *Int. Rev. Cyt.* **189,** 267–301 (1999).
10. Borejdo, J., Talenta, J., Akopova, I. & Burghardt, T. P. Rotations of a few cross-bridges in muscle by confocal total internal reflection microscopy. *Biochim. Biophys. Acta* **1763,** 137–140 (2006).
11. Nihei, T., Mendelson, R. A. & Botts, J. Use of fluorescence polarization to observe changes in attitude of S1 moieties in muscle fibers. *Biophys. J.* **14**, 236–242 (1974).
12. Borejdo, J. & Putnam, S. Polarization of fluorescence from single skinned glycerinated rabbit psoas fibers in rigor and relaxation. *Biochem. Biophys. Acta* **459**, 578–595 (1977).
13. Borovikov, Y. S., Kuleva, N. V. & Khoroshev, M. I. Polarization microfluorimetry study of interaction between myosin head and F-actin in muscle fibers. *Gen. Physiol. Biophys.* **10,** 441–459 (1991).
14. Berger, C. L., Craik, J. S., Trentham, D. R., Corrie, J. E. & Goldman, Y. E. Fluorescence polarization of skeletal muscle fibers labeled with rhodamine isomers on the myosin heavy chain. *Biophys. J.* **71**, 3330–3343 (1996).

15. Irving, M. *et al.* Tilting of the light-chain region of myosin during step length changes and active force generation in skeletal muscle. *Nature* **375**, 688-691 (1995).
16. Corrie, J. E. T. *et al.* Dynamic measurement of myosin light-chain-domain tilt and twist in muscle contraction. *Nature* **400**, 425-430 (1999).
17. Borovikov, Y. S. *et al.* Behavior of caldesmon upon interaction of thin filaments with myosin subfragment 1 in ghost fibers. *Biochim. Biophys. Acta* **689,** 183–189 (2004).
18. Nowak, E., Borovikov, Y. S., Khoroshev, M. I. & Dabrowska, R. Troponin I and caldesmon restrict alterations in actin structure occurring on binding of myosin subfragment 1. *FEBS Lett.* **281,** 51–54 (1991).
19. Kulikova, N., Pronina, O. E., Dabrowska, R. & Borovikov, Y. S. Caldesmon inhibits the actin-myosin interaction by changing its spatial orientation and mobility during the ATPase activity cycle. *Biochem. Biophys. Res. Commun.* **357**, 461-466 (2007).
20. Borovikov, Y. S., Moraczewska, J., Khoroshev, M. I. & Strzelecka-Gołaszewska, H. Proteolytic cleavage of actin within the DNase-I-binding loop changes the conformation of F-actin and its sensitivity to myosin binding. *Biochim. Biophys. Acta* **1478**, 138-1351 (2000).
21. Borovikov, Y. S. *et al.* Caldesmon freezes the structure of actin filaments during the actomyosin ATPase cycle. *Biochim. Biophys. Acta* **1764**, 1054–1062 (2006).
22. Lamkin, M., Tao, T. & Lehrer, S. S. Tropomyosin–troponin and tropomyosin–actin interactions: a fluorescence quenching study. *Biochemistry* **22,** 3053–3058 (1983).
23. Andreev, O. A., Takashi, R. & Borejdo, J. Fluorescence polarization study of the rigor complexes formed at different degrees of saturation of actin filamentswith myosin subfragment-1. *J. Muscle Res. Cell Motil.* **16,** 353–367 (1995).
24. Ohki, T., Mikhailenko, S. V., Morales, M. F., Onishi, H. & Mochizuki, N. Transmission of force and displacement within the myosin molecule. *Biochemistry* **43**, 13707–13714 (2004).
25. Rayment, I. *et al.* Structure of the actin-myosin complex and its implications for muscle contraction. *Science* **261**, 58-65 (1993).
26. Holmes, K. C., Angert, I., Jon Kull, F., Jahn, W. & Schröder, R. R. Electron cryo-microscopy shows how strong binding of myosin to actin releases nucleotide. *Nature* **425**, 423-427 (2003).
27. Kad, N. M., Patlak, J. B., Fagnant, P. M., Trybus, K. M. & Warshaw, D. M. Mutation of a conserved glycine in the SH1-SH2 helix affects the load-dependent kinetics of myosin. *Biophys. J.*, **92**, 1623-1631 (2007).
28. Onishi, H. & Morales, M. F. A closer look at energy transduction in muscle. *PNAS* **104**, 12714–12719 (2007).
29. Borejdo, J. *et al.* Changes in orientation of actin during contraction of muscle. *Biophys. J.* **86**, 2308-2317 (2004).
30. Borejdo, J., Muthu, P., Talent, J., Akopova, I. & Burghardt, T. P. Rotation of actin monomers during isometric contraction of skeletal muscle. *J. Biomed. Opt.* **121**, 014013 (2007).
31. Bremel, R. D., Murray, J. M. & Weber, A. Manifestations of cooperative behavior in the regulated actin filament during actin-activated ATP hydrolysis in the presence of calcium. *Cold Spring Hbr. Symp. Quant. Biol.* **37**, 267–275 (1972).
32. Murray, J. M., Knox, M. K., Trueblood, C. E. & Weber, A. Do tropomyosin and myosin compete for actin sites in the presence of calcium? *FEBS Lett.* **114**, 169–173 (1980).
33. Bing, W., Knott, A. & Marston, S. B. A simple method for measuring the relative force exerted by myosin on actin filaments in the in vitro motility assay: evidence that tropomyosin and troponin increase force in single thin filaments. *Biochem. J.* **350**, 693–699 (2000).
34. Fujita, H., Lu, X., Suzuki, M., Ishiwata, S. & Kawai, M. The effect of tropomyosin on force and elementary steps of the cross-bridge cycle in reconstituted bovine myocardium. *J. Physiol.* **556**, 637–649 (2004).
35. Cooke, R. The mechanism of muscle contraction. *CRC Crit. Rev. Biochem.* **21**, 53-118 (1986).

36. Holmes, K. C. The swinging lever-arm hypothesis of muscle contraction. *Curr. Biol.* **7**, 112-118 (1997).
37. Lu, X., Tobacman, L. S. & Kawai, M. Temperature-dependence of isometric tension and cross-bridge kinetics of cardiac muscle fibers reconstituted with a tropomyosin internal deletion mutant. *Biophys. J.* **91**, 4230-4240 (2006).
38. Holthauzen, L. M. F., Corrêa, F. & Farah, C. S. Ca^{2+}-induced rolling of tropomyosin in muscle thin filaments. *JBC* **279**, 15204–15213 (2004).
39. Borovikov, Y. S. & Gusev, N. B. Effect of troponin–tropomyosin complex and Ca^{2+} on conformational changes in F-actin induced by myosin subfragment-1. *Eur. J. Biochem.* **136,** 363–369 (1983).
40. Borovikov, Y. S., Nowak, E., Khoroshev, M. I. & Dabrowska, R. The effect of Ca^{2+} on the conformation of tropomyosin and actin in regulated actin filaments with or without bound myosin subfragment 1. *Biochim. Biophys. Acta* **1163**, 280-286 (1993).
41. Huxley, A. F. Muscle structure and theories of contraction. *Prog Biophys Biophys Chem.* **7**, 255-318 (1957).
42. Miki, M., dos Remedios, C. G. & Barden, I. A. Spatial relationship between the nucleotide-binding site, Lys-61 and Cys-374 in actin and a conformational change induced by myosin subfragment-1 binding. *Eur. J. Biochem.* **168,** 339-345 (1987).
43. Tregear, R. & Mendelson, R. A. Polarization from a helix of fluorophores and its relation to that obtained from muscle. *Biophys. J.* **15**, 455–467 (1975).
44. Goody, R. S. & Hofmann, W. Stereochemical aspects of the interaction of myosin and actomyosin with nucleotides. *J. Muscle Res. Cell Motil.* **1**, 101–115 (1980).
45. Roopnarine, O. & Thomas, D. D. Orientation of intermediate nucleotide states of indane dione spin-labeled myosin heads in muscle fibers. *Biophys. J.* **70**, 2795–2806 (1996).
46. Okamoto, Y. & Sekine, T. A streamlined method of subfragment one preparation from myosin. *J. Biochem. (Tokyo)* **98,** 1143–1145 (1985).
47. Spudich, J. A. & Watt, S. The regulation of rabbit skeletal muscle contraction. 1. Biochemical studies of the interaction of the tropomyosin-troponin complex with actin and the proteolytic fragments of myosin. *J. Biol. Chem.* **246,** 4866-4871 (1971).
48. Robinson, P. *et al.* Mutations in fast skeletal troponin I, troponin T, and beta-tropomyosin that cause distal arthrogryposis all increase contractile function. *FASEB J.* **21,** 896-905 (2007).
49. Szent-Gyorgyi, A. G. Meromyosins, the subunits of myosin. *Arch. Biochem. Biophys.* **42,** 305 (1953).

Supplementary Information

Author Information The authors declare no competing financial interests. Correspondence and requests for materials should be addressed to Y.S.B. (boroviko@mail.cytspb.rssi.ru).

Full Methods

Myosin subfragment-1 (S1) devoid of regulatory light chains was prepared by treatment of the skeletal muscle myosin with α-chymotrypsin for 10 min at 25°C[46]. Modification of the reactive Cys707 of S1 with 1.5-IAEDANS was carried out in a method described by Borejdo and Putnam[12]. The degree of labeling was of 0.9–0.95. Skeletal muscle actin was isolated from acetone-dried muscle powder and purified as described by Spudich and Watt[47]. Labeling of actin with N-iodoacetyl-N'-(5-sulpho-1-naphthyl)ethylenediamine (1.5-IAEDANS) at Cys374 was performed as described by Miki et al.[42]. Recombinant wile type human αα- and ββ-tropomyosin and troponin subunits were overexpressed as previously described[48]. Whole troponin complex was formed using the established protocol[48]. Labeling of tropomyosin with 5-IAF at Cys36 or Cys190 was performed as described[22] at probe to protein ratio 0.8:1.

Glycerinated muscle fibers were obtained from rabbit *psoas* muscles by the method of Szent-Gyorgyi[49]. Ghost fibers were prepared by incubation of single glycerinated fibers for 1.5 h in a solution containing 800 mM KCl, 1 mM $MgCl_2$, 10 mM ATP, 67 mM phosphate buffer, pH 7.0 as described earlier[39]. The resultant ghost fibers were composed by more than 80% of actin. S1, tropomyosin and troponin were added to thin filaments by incubation in the solution containing 20 mM KCl, 1 mM $MgCl_2$, 1 mM DTT, 10 mM Tris-HCl, pH 6.8 and 1-2.5 mg/ml protein. The sequence of the incorporation of proteins into the ghost fibers was as follows: S1, tropomyosin, troponin. The unbound proteins were washed out by incubation of the fibers in the same buffer without proteins. In some experiments 1.5-IAEDANS labeled G-actin was incorporated in ghost fibers. The reconstruction of filaments from exogenous G-actin within the fibers was performed as described earlier[20]. The molar ratio of the corresponding protein to actin was determined by SDS-PAGE with subsequent densitometry of the gels (UltroScan XL, Pharmacia LKB). The molar ratio of S1, tropomyosin and troponin to actin was 1:5 (±2), 1:6.5 (±2) and 1:6.5 (±1), respectively.

The polarized fluorescence from 1.5-IAEDANS-labeled S1, 1.5-IAEDANS-labeled actin and 5-IAF-labeled TM was registered at 500–600 nm after excitation at 365±5 nm and 437±5 nm, respectively. The measurement were carried out in the buffer containing 10 mM KCl, 3 mM $MgCl_2$, 1 mM DTT, 4 mM EGTA (or 0.1 mM $CaCl_2$), 6.7 mM phosphate buffer, pH 7.0, in the absence or presence of 2.5 mM ADP, 25 mM AMP-PNP, 10 mM ATPγS or 5 mM ATP[21]. The absence of the nucleotide modeled the AM state of the actomyosin complex. MgADP, MgAMP-PNP, MgATPγS and MgATP were used for modeling of the intermediate states of actomyosin, AM^·ADP, AM**·ADP·Pi and AM*·ATP, respectively[44,45], where A is actin and M, M*, M** and M^ are various conformational states of the myosin head. The intensities of the four components of polarized fluorescence were measured parallel ($_{\parallel}I_{\parallel}$, $_{\parallel}I_{\perp}$) and in perpendicular ($_{\perp}I_{\perp}$, $_{\perp}I_{\parallel}$) to the fiber axis relative to the polarization plane of the exiting light using a photometer[17]. Fluorescence polarization ratios were defined as: $P_{\parallel} = (_{\parallel}I_{\parallel} - _{\parallel}I_{\perp})/(_{\parallel}I_{\parallel} + _{\parallel}I_{\perp})$ and $P_{\perp} = (_{\perp}I_{\perp} - _{\perp}I_{\parallel})/(_{\perp}I_{\perp} + _{\perp}I_{\parallel})$.

To estimate the changes in a probe orientation we used the model-dependent and model-independent methods[17,43], in view of the ordered probes lies at angles Φ_A and Φ_E with respect to fiber axis for absorption ($\vec{A}$) and emission ($\vec{E}$) dipoles, respectively and N is completely disordered probes. The thin filament was assumed to be rigid; the angle between the fiber axis and the thin filament axis was assumed to be zero. The statistical reliability of the changes was evaluated using Student's t-test.

IAEDANS-S1

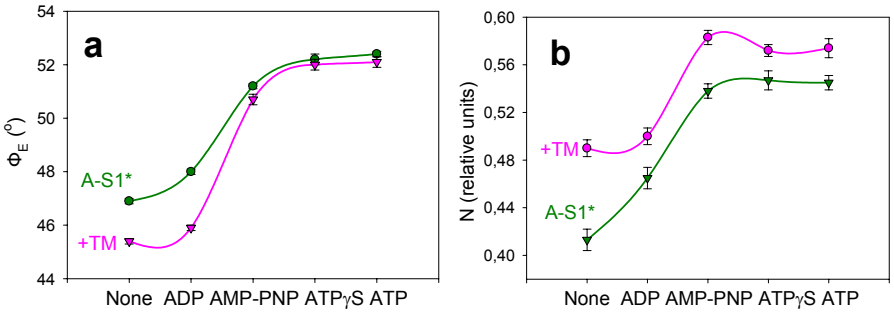

IAEDANS-Actin

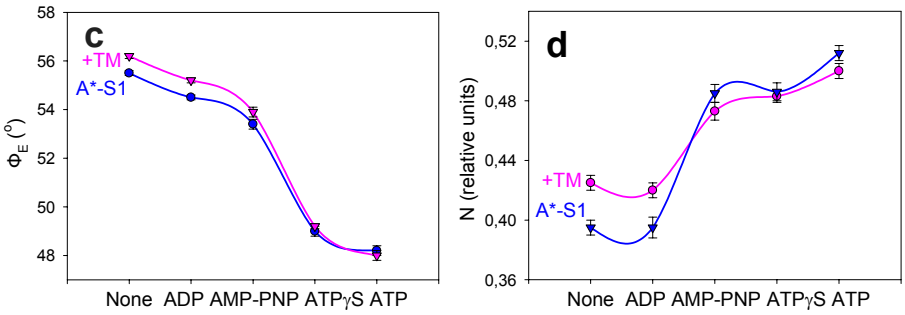

IAF-TM

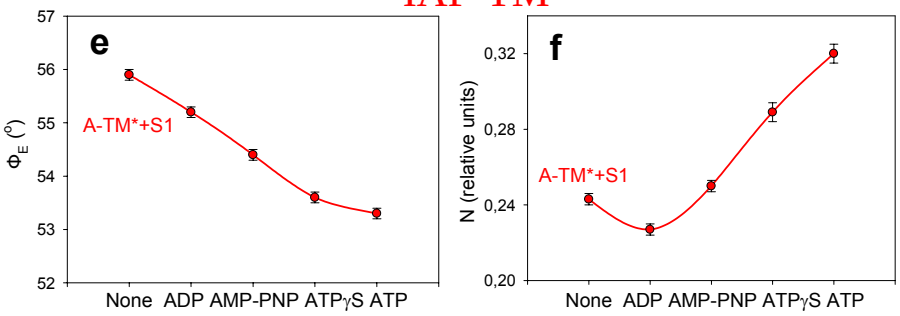

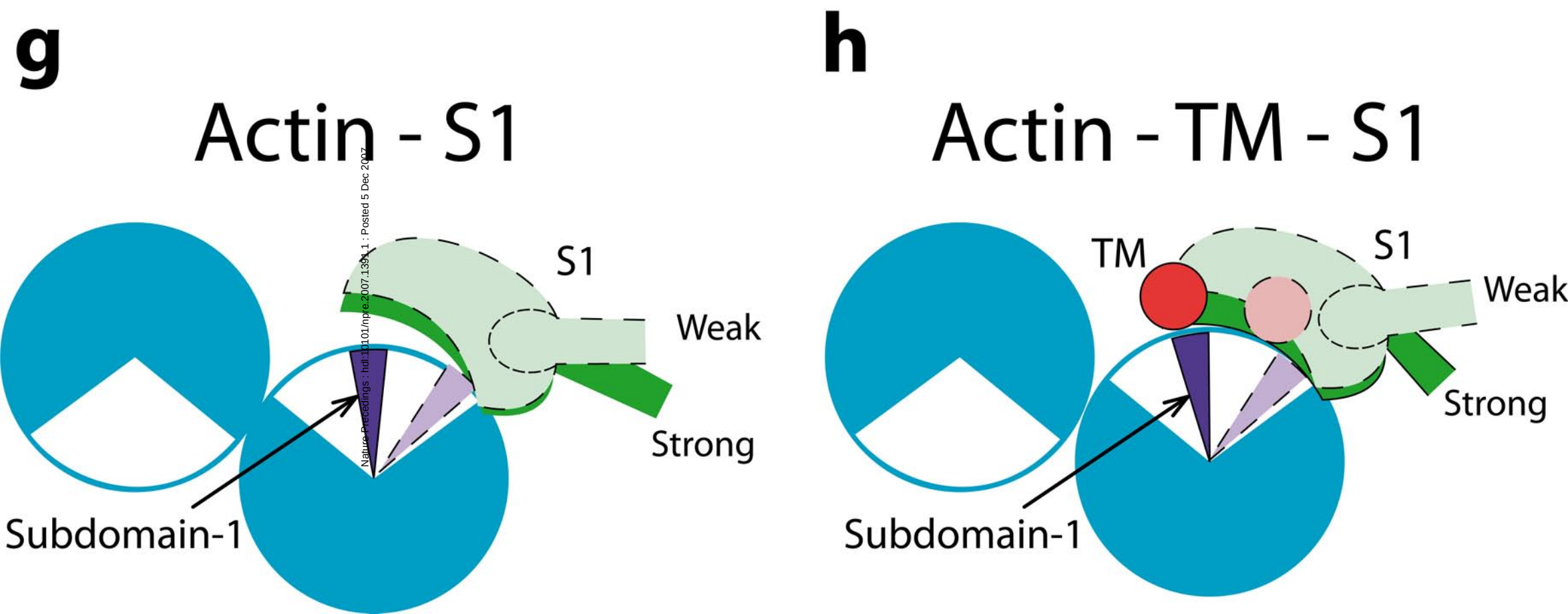

IAEDANS-S1

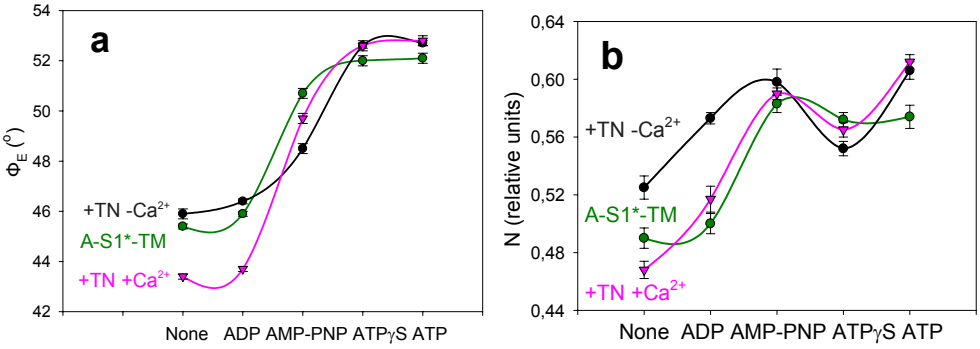

IAEDANS-Actin

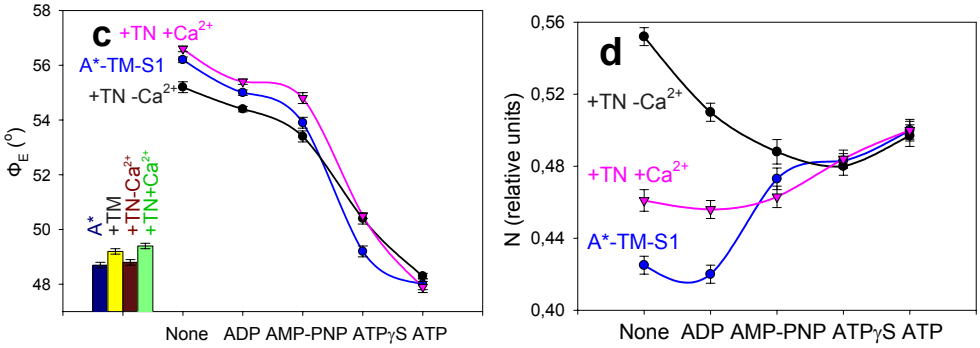

IAF-TM

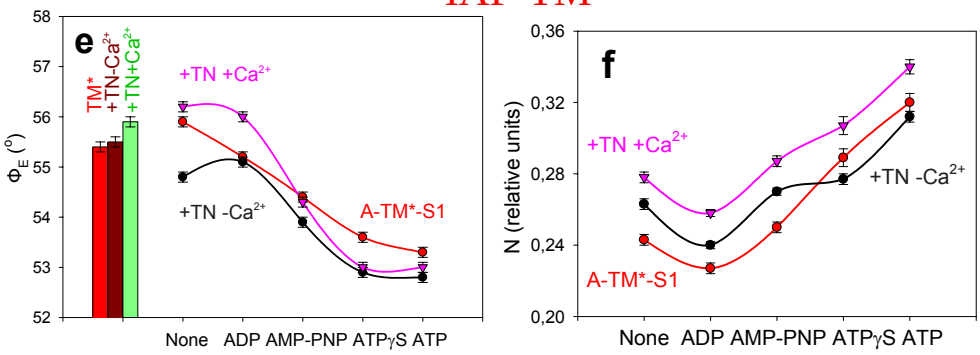

g

Actin-TM-S1-TN +Ca^{2+}

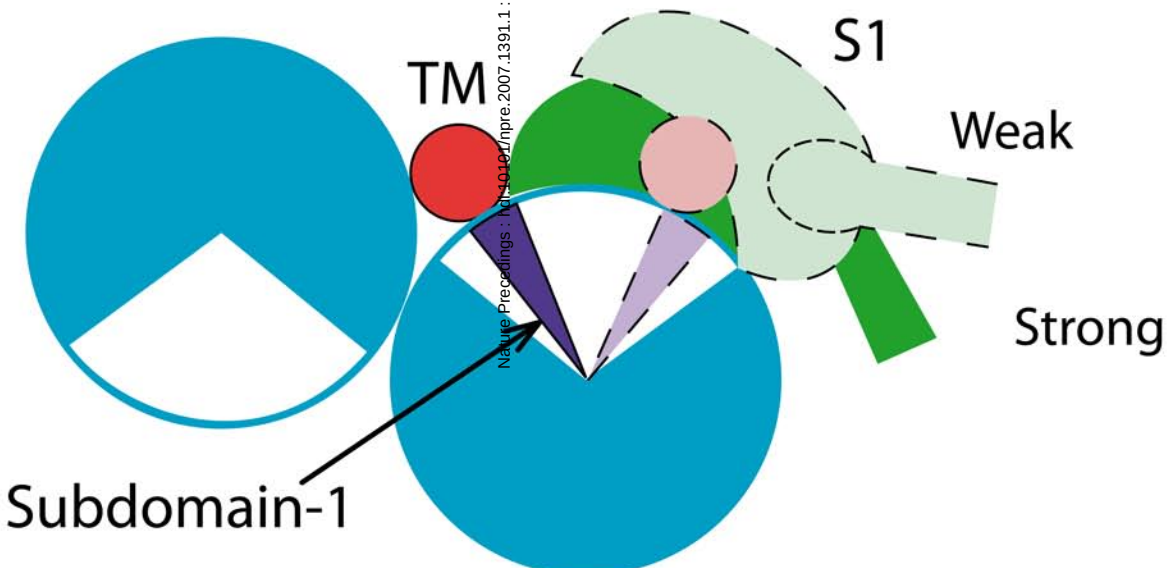

h

Actin-TM-S1-TN -Ca^{2+}